J Mol Model (2013) 19:4395–4402
DOI 10.1007/s00894-013-1950-5

ORIGINAL PAPER

Theoretical study on the adsorption of phenol on activated carbon using density functional theory

Le Minh Cam · Le Van Khu · Nguyen Ngoc Ha

Received: 4 May 2013 / Accepted: 16 July 2013 / Published online: 6 August 2013

Abstract Density functional theory (DFT) calculations performed at the PBE/DZP level using the DFT-D2 method were utilized to investigate the adsorption of phenol on pristine activated carbon (AC) and on activated carbon functionalized with OH, CHO, or COOH groups. Over the pristine AC, the phenol molecule undergoes weak physical adsorption due to van der Waals interactions between the aromatic part of the phenol and the basal planes of the AC. Among the three functional groups used to functionalize the AC, the carboxylic group was found to interact most strongly with the hydroxyl group of phenol. These results suggest that functionalized AC-COOH has great potential for use in environmental applications as an adsorbent of phenol molecules in aqueous phases.

Keywords Activated carbon (AC) · Phenol (Ph-OH) · DFT · Adsorption

Introduction

The removal of pollutants from industrial waters and wastewaters emerged as an important concern during the last decade. However, the effective degradation of these pollutants has become a challenging task due to environmental laws. Among the various organic pollutants that are found in water, phenol and phenolic compounds have received increased attention in recent years due to their high toxicity [1]. Traditionally, biological treatment [2], activated carbon adsorption [3, 4], reverse osmosis [5], ion exchange [6], solvent extraction [7], and chemical oxidation [8] have been used to remove pollutants. Among these, adsorption has been effectively used for the removal of organic as well as inorganic compounds from wastewater because of its simplicity and safety [1].

L. M. Cam (✉) · L. Van Khu · N. N. Ha
The University of Education, Hanoi, Vietnam
e-mail: camlm@hnue.edu.vn

Activated carbon (AC), which has high surface area, a large pore volume, and a broad pore size distribution, is one of the most useful adsorbents that can be used in liquid-phase adsorption processes [9]. The surface chemistry of the carbon is dictated by the heteroatoms (such as oxygen, nitrogen, hydrogen, and phosphorus) present on it [10, 11]. Those heteroatoms represent organic functional groups at the edges of carbon crystallites. The heteroelement content of the carbon depends on its origin and the activation method employed [12]. The presence of the heteroatoms also has a significant effect on the adsorption of polar species. When functional groups are present, molecules that interact with the carbon in a specific way will be adsorbed more strongly and more of them will be adsorbed [13] compared to adsorption on pure carbon layers. Moreover, heteroatoms can catalytically influence the conversion of adsorbed species [14, 15] or they can physically hinder the adsorption of nonpolar molecules [16].

In recent years, there have been numerous experimental studies of the adsorption of phenol on active carbon [17–19]. This adsorption process depends on several factors, which include the nature of the adsorbent, the adsorbate, and the adsorption conditions. Relevant adsorbent characteristics include the surface area, pore size distribution, hydrophobicity, and the density and type of functional groups present on the surface. The nature of the adsorbate refers to its polarity, its hydrophobicity, the size of the molecule, and its acidity or basicity (which is determined by the nature of the functional group present, if any). Adsorption conditions include the temperature, the polarity of the solvent (when applicable), and the presence of other species that compete for the adsorption sites [17]. Leng and Pinto [18] have found that the uptake of phenol is a combined effect of physisorption and surface polymerization, where physisorption is the interaction of the phenol with the basal planes of carbon. They found out that the functional groups on the activated carbon play roles in both the electrostatic and the dispersive interactions.

To our knowledge, few theoretical studies on the adsorption of phenol on AC surfaces have been reported. It is important to understand the advantages and disadvantages of phenol adsorption on AC when utilizing this adsorption to remove phenol from water in other applications. Determining the structural properties of the adsorbed phenol on the surface is also important as it leads to a better understanding of its bonding and reactivity during catalysis. Density functional theory (DFT) is widely applied in molecular modeling studies to predict and display structures, spectroscopic parameters, and energy changes of small, medium-sized, and large molecules in chemistry. The successful combination of theoretical calculations and practical results allows deep insight into the problem being studied and improves our understanding of the phenomenon under investigation. In this paper, we report the results of density functional calculations of the adsorption of an isolated phenol molecule on the outer surface of AC. The capacities of pristine and modified AC to adsorb and thus remove phenol were evaluated.

Model and methods

Modeling the activated carbon surface

The most important prerequisite for a theoretical study of reactions occurring in the presence of activated carbon, an amorphous material, is to know the correct atomic structure of activated carbon. Much research has been conducted to determine the structure of carbon produced by the pyrolysis of organic materials. The first attempt was made by Rosalind Franklin in the 1950s [20]. She showed that the carbon from which activated carbon is derived is "non-graphitizing," meaning that it cannot be transformed into crystalline graphite even at temperatures of 3000 °C and above. Franklin built up a simple model of non-graphitizing carbon in which small graphitic crystallites were joined together by crosslinks, but did not explain the nature of these crosslinks. A much more recent suggestion [21, 22] was that non-graphitizing carbon has a structure related to that of the fullerenes; in other words, it consists of curved fragments containing pentagons and other non-hexagonal rings in addition to hexagons. Both X-ray and neutron diffraction have been applied to study non-graphitizing carbons, and in some of these studies the diffraction data were interpreted as demonstrating a structure containing non-haxagonal rings [23, 24]. The most recent study done by Harris et al. [25] used aberration-corrected transmission electron microscopy (TEM) to image the atomic structure of a commercial activated carbon. Atomic-resolution images of both the as-produced carbon and the carbon following heat treatment at 2000 °C were recorded. Images of the fresh carbon contained evidence of hexagonal rings, and possibly non-hexagonal ones. There was also strong evidence in some of the images for the presence of pentagonal rings (Fig. 1). The presence of pentagons in the heat-treated carbon strongly suggested that such rings were present in the orginal carbon. Heat treatment of the fresh carbon apparently increased the size of the hexagonal network but left many of the pentagons intact. Therefore, their results supported the previous idea that this type of carbon has a fullerene-related structure. Such a structure would help to explain the microporosity and many other properties of non-graphitizing carbon.

Theoretical studies on adsorption on activated carbon are very rare. Wilcox et al. [26] theoretically examined how different functional groups and halogens on the surface of activated carbon affect elemental mercury using DFT theory. However, for their theoretical model, the authors assumed that the molecular framework of activated carbon is similar to that of graphite. Pyrene, with four fused rings, was employed as a representative cluster species to model the activated carbon surface. Some theoretical studies of graphite [27–32] have confirmed that most of its physics is the same as that of a single graphite layer. Traditionally, in theoretical studies, the structural models that are used to simulate adsorption are derived from graphite, in which all the atoms are in hexagonal rings [33]. The carbon pores are then assumed to have a slit-like shape confined by the parallel planes of the graphite. However, some theoretical studies have already been carried out which show that a model structure containing fullerene-related elements provides a better basis for understanding adsorption on activated carbon than the traditional models [34, 35].

Therefore, in this study, the fullerene-related structure was chosen for the theoretical model of activated carbon. The model was a $C_{45}H_{15}$ cluster containing one pentagonal and fifteen hexagonal rings (Fig. 2).

Computational methodology

All quantum calculations were performed using the DFT method with nonlocal, gradient-corrected DFT. The Perdew, Burke, and Ernzerhof (PBE) gradient-corrected functional [36] was employed in the calculation of the exchange-correlation energy. The double-zeta plus polarization (DZP) basis set was used for all atoms; this is known to be sufficiently accurate for hydrogen-bonding calculations. Geometry optimization of all equilibrium structures was performed until the forces acting on the dynamic atoms were all smaller than 0.002 Ha/Å.

To take into account water solvation effects, the conductor-like screening model [37] (COSMO) was applied. This is a continuum solvation model where the solute molecule forms a cavity within the dielectric continuum of permittivity ε that represents the solvent. The charge distribution of the solute polarizes the dielectric medium. The response of the medium is described by the generation of screening charges on the cavity surface. COSMO derives the polarization charges of

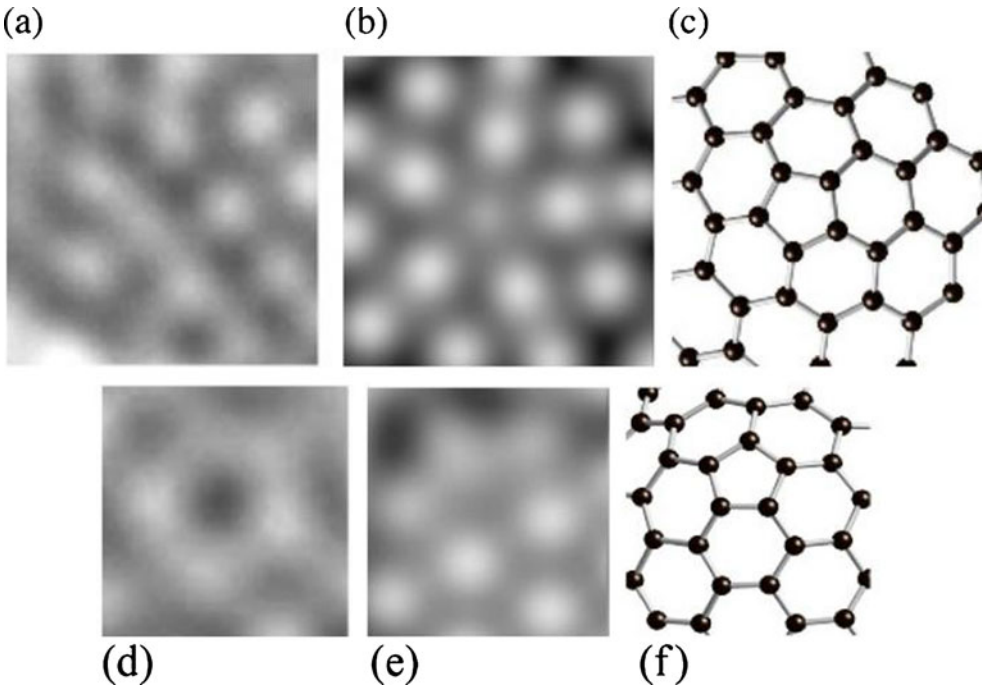

Fig. 1a–f Aberration-corrected TEM of activated carbon. **a** Enlargement showing a pentagonal arrangement of spots. **b** Simulated image of the structure shown in **c**. **d** Second region showing a pentagonal arrangement. **e** Simulated image of the structure shown in **f**. Images are from [25]

the continuum, caused by the polarity of the solute, using a scaled-conductor approximation. If the solvent was an ideal conductor, the electric potential on the cavity surface would disappear. If the distribution of the electric charge in the molecule is known (e.g., from quantum chemistry), then it is possible to calculate the charge q^* on the surface segments. For solvents with finite dielectric constants, this charge q is approximately a factor $f(\varepsilon)$ smaller:

$$q = f(\varepsilon).q^*. \tag{1}$$

The factor $f(\varepsilon)$ is approximately

$$f(\varepsilon) = \frac{\varepsilon - 1}{\varepsilon + x}, \tag{2}$$

where the value of x is set to 0.5 based on theoretical arguments. Some re-implementations of COSMO use x=0. The energy of the interaction between the solvent and the solute molecule can be calculated from the thus determined solvent charges q and the known charge distribution of the molecule.

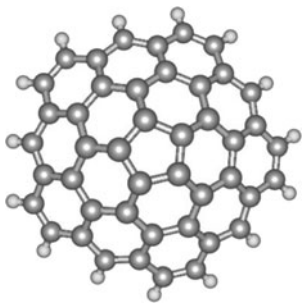

Fig. 2 Selected model of the activated carbon surface

Noncovalent forces, such as hydrogen bonding and van der Waals (vdW) interactions, are crucial for the formation, stability, and function of molecules and materials. A pragmatic method of working around this problem is provided by the DFT-D approach [38], which consists of adding a semi-empirical dispersion potential to the conventional Kohn–Sham DFT energy:

$$E_{\mathrm{DFT-D}} = E_{\mathrm{KS-DFT}} + E_{\mathrm{disp}}. \tag{3}$$

In the DFT-D2 method of Grimme [39], the van der Waals interactions are described by a simple pair-wise force field that is optimized for several popular DFT functionals. The dispersion energy is defined as

$$E_{\mathrm{disp}} = -s_6 \sum_{i<j} \frac{C_6^{ij}}{r_{ij}^6} \frac{1}{1 + \mathrm{e}^{-d\left(r_{ij} \Big/ s_R R_{ij} - 1\right)}}, \tag{4}$$

where r_{ij} is the distance between the i-th and the j th atoms. The prefactor s_6 is a fitted scaling parameter that is material independent but different for each version of GGA. The coefficients C_6^{ij} introduce another degree of empiricism through the constants C_6^{i}, which are tabulated for each element in the periodic table. Finally, the parameters $R_{ij} = R_i + R_j$ combine the tabulated emprical van der Waals radii R_i, which are used with the constants d and s_R to determine the behavior of the damping function.

Results and discussion

In principle, there are a number of ways in which phenol may bind to the surface of the active carbon (AC). However, according to the molecular electrostatic potential surface (MEP) of phenol, the oxygen atom (−0.687) and aromatic ring (−0.261) of the phenol molecule are negatively charged, so there are two different ways in which phenol can interact with the surface of the adsorbent: via its hydroxyl group –(O_{ph}–H_{ph}) or via the aromatic ring (AR).

Phenol adsorption on pristine AC

For the starting configuration, the phenol molecule was located in front of the AC surface with the –(O_{ph}–H_{ph}) group oriented perpendicularly and end-on at the center site above the hexagon or with the aromatic ring oriented parallel to and above the hexagon. Because the AC surface was assumed to consist of curved fragments, phenol can approach the surface carbon atoms from two sides: the convex side (C_{cv}) and the concave side (C_{cc}). Starting from the C_6H_5OH + C(AC) system, four modes of interactions were studied: (O_{ph}–H_{ph})···C_{cv}(AC); (O_{ph}–H_{ph})···C_{cc}(AC); (AR)···C_{cv}(AC); and (AR)···C_{cc}(AC).

Initial configurations were studied using the optimized energy method (the quasi-Newton method). The convergence threshold was assumed to be reached when the force was 0.03 eV/Å. Adsorption energies E_{ads} (or interaction energies) were calculated via

$$E_{ads} = E(C_6H_5OH + AC) - E(C_6H_5OH) - E(AC). \quad (5)$$

Final configurations are shown in Fig. 3: a and b illustrate the adsorption of phenol on the concave side, whereas c and d show the adsorption of phenol on the convex side. Each image indicates the shortest distance between Ph-OH and AC: the (O_{ph}–H_{ph})···C_{cv}(AC) distance was 2.602 Å; the (O_{ph}–H_{ph})···C_{cc}(AC) distance was 3.149 Å; the distance between AR and C_{cv}(AC) was 3.293 Å; and a value of 2.642 Å was found for the AR···C_{cc}(AC) distance. Clearly, the bonding associated with the four complexes does not appear to be as strong as that associated with chemisorption.

From Table 1, it can be seen that the final adsorption energies are quite low, ranging from −6.731 to −15.198 kJ/mol^{-1}, except in the last case (aromatic ring attached to the concave side of the graphite layer), which has an adsorption energy of −108.28 kJ/mol^{-1}. Indeed, the small E_{ads} values and long Ph···AC distances suggest that phenol molecules are not

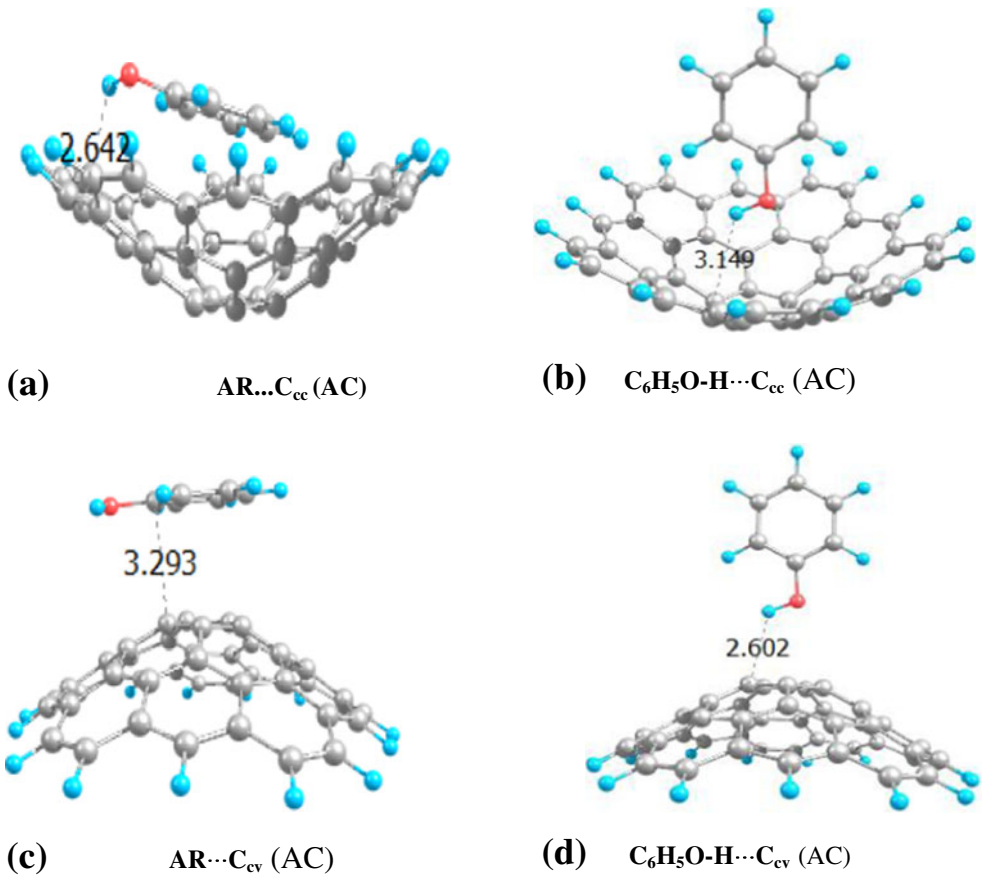

Fig. 3a–d Four optimized structures for the adsorption of phenol on pristine AC (**a** and **b** illustrate the adsorption of phenol on the concave side, whereas **c** and **d** show the adsorption of phenol on the convex side of the AC layer)

significantly adsorbed at such active sites, and only undergo weak physical adsorption on pristine AC due to weak van der Waals interactions between the AC surface and the phenol molecules.

Our calculated results revealed that the main contributor to the negative values of E_{ads} obtained was the dispersion energy. When the dispersion energy was not taken into account, all of the adsorption energies became positive, indicating a repulsive interaction between the phenol molecule and the surface of pristine AC, which means that the interaction between phenol and pure activated carbon is unfavorable.

The same results were reported by Zhao and coworkers for adsorption on a SiCNT (carbon nanotube) [40], and by Peyghan and coworkers [41] and Rokhina et al. [42]. Zhao's results showed that the hydroxyl group of phenol interacts with the adsorbent much more strongly than its aromatic ring does. Peyghan et al. [41] studied the adsorption of phenol on pure (4,4) armchair single-walled boron nitride nanotubes (BNNTs), and concluded that pure BNNTs cannot significantly detect phenol molecules because they cannot be completely adsorbed on the surface. Rokhina et al. [42] studied acid-functionalized carbon nanofibers (CNFs) and showed that pristine nanofibers do not have any capacity to adsorb phenol.

With its high adsorption energy of −108.28 kJ/mol^{-1}, the adsorption of phenol on cavities in the AC (the concave side of the graphite layer in our study) is the most favorable interaction mode. This may result from the very large contact area between the phenol molecule and the AC surface in this case, maximizing the van der Waals interactions (according to Eq. 4, the van der Waals energy is inversely proportional to the distance r_{ij} between the ith and the jth atoms).

Phenol adsorption on the functionalized AC surface

The adsorption of phenol molecules on pristine AC is highly disfavored. This is probably due to the high hydrophobicity of the surface and/or the absence of an appropriate functional group on the surface with which to interact, as such groups play a major role in the phenol adsorption mechanism [42].

Table 1 Adsorption energies (in kJ/mol^{-1}) of optimized structures (C_6H_5OH + C(AC) system)

	C_6H_5O-H···C_{cv}	C_6H_5O-H···C_{cc}	AR···C_{cv}	AR···C_{cc}
E_{ads} (including the dispersion energy)	−15.198	−3.726	−6.731	−108.28
E_{ads} (without the dispersion energy)	7.199	11.600	8.526	18.399
Phenol...C(AC) distance (Å)	2.602	3.149	3.293	2.642

Actually, the surface of AC always contains functional groups such as –OH, –CH=O, and –COOH, especially when AC has been treated with an oxidizing agent such as HNO_3, H_2O_2, or $(NH_4)_2S_2O_8$ [43]. Surface treatment with nitric acid can introduce hydroxyl, carboxylic, and carboxylic anhydride groups [44]. The presence of a carboxylic group (electron-withdrawing group) on the aromatic ring lowers its electronic density and thus allows the aromatic ring to act as an electron acceptor. In order to determine how the presence of each functional group influences the adsorption capacity of the AC, the adsorption of a phenol molecule onto various functionalized AC surfaces was investigated.

A model of AC-X (X = –OH, –CH=O, –COOH) was built up by replacing a pentagonal ring located at the top of the convex side with an –X group. Hydrogen atoms were used to saturate the edges of the AC layer. The interactions of the phenol molecule with the functionalized AC surface, including hydrogen bonding between the OH group of phenol and the oxygen atom of the functional group on AC or between the OH of X and the oxygen atom of phenol, were then investigated.

Phenol adsorption on (AC)-OH

Starting from the C_6H_5OH + (AC)-OH system, two modes of interactions were studied: (C_6H_5)OH···OH(AC) and (C_6H_5)HO···HO(AC).

The optimized geometries of phenol adsorption on (AC)-OH are shown in Fig. 4, and the corresponding adsorption energies are shown in Table 2. The values shown are the shortest distances between the phenol molecule and the AC surface. A comparison of the two configurations leads to the following comments:

The **(C_6H_5)OH···OH(AC) interaction** was less favorable, with a weak adsorption energy of 8.291 kJ/mol^{-1}. Although the H–O bond length of phenol slightly elongated from 0.982 Å to 0.986 Å, the H–O bond distance of (AC)OH was almost unchanged. The (C_6H_5)OH···OH(AC) distance was 1.908 Å. Such a large distance clearly demonstrates that the interaction between the OH group of the phenol molecule and the oxygen atom in HO-AC is not significant. The **(C_6H_5)HO···HO(AC) interaction** was more favorable and resulted in a stable complex due to a more negative adsorption energy (E_{ads} = −30.736 kJ/mol^{-1}). Moreover, the distance between the H atom of the OH group in (AC)-OH and the O atom of the OH group in phenol was 1.689 Å (which is shorter than that in the (C_6H_5)OH···OH(AC) interaction). A redshifted hydrogen bond appeared in this interaction mode because the length of the H–O bond in (AC)-OH increased from 0.984 Å to 1.004 Å. The harmonic hydroxyl stretching frequency

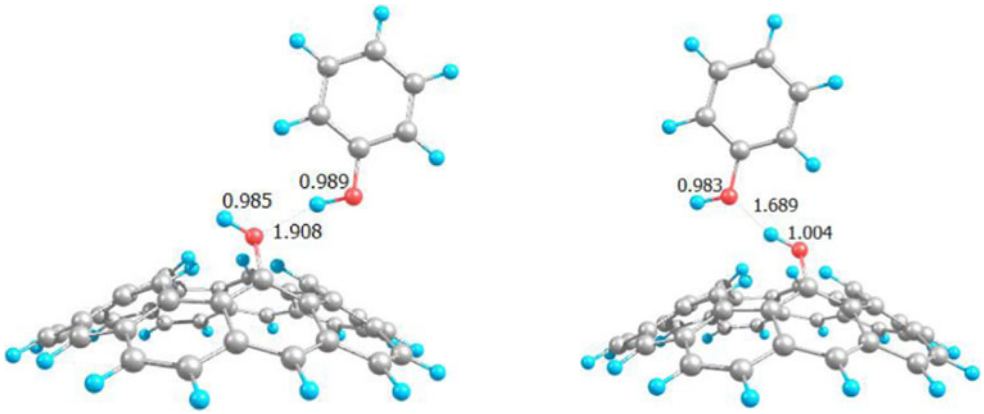

Fig. 4 Optimized structures for phenol adsorption on (AC)-OH

shifted from 3,592 cm^{-1} to 3181.6 cm^{-1} as the $(C_6H_5)HO\cdots HO(AC)$ complex was formed.

The favorability of the $(C_6H_5)HO\cdots HO(AC)$ interaction can also be explained by the stronger acidity of the H atom in the O–H group of (AC)-OH in comparison to that of C_6H_5OH. This is proven by the difference in the H–O bond lengths: in (AC)-OH, the H–O bond distance is 0.984 Å, which is longer than the H–O bond distance in the phenol molecule (0.982 Å). This corresponds to a smaller harmonic hydroxyl stretching frequency for (AC)-OH compared to that for C_6H_5OH (see Table 3). In addition, the positive charge on the H atom of the OH group in (AC)-OH is +0.461, whereas that for C_6H_5OH is +0.453.

Phenol adsorption on (AC)-CHO

The calculated results revealed that, for the C_6H_5OH + (AC)-CHO system, only one kind of hydrogen bond occurs when C_6H_5OH reacts with (AC)-CHO to form the $(C_6H_5)OH\cdots OCH(AC)$ complex. This configuration results from an interaction between the H atom in the OH group of C_6H_5OH and the oxygen atom in the CHO group of (AC)-CHO. Due to this interaction, the O–H bond of C_6H_5OH weakens and increases in length from 0.982 Å to 0.999 Å. Due to this increase in the O–H bond distance, the hydroxyl stretching frequency of C_6H_5OH decreases from 3634.6 cm^{-1} to 3286.0 cm^{-1}. The distance between the oxygen atom of the CHO group and the H atom in the OH group is 1.803 Å, indicating a weak van der Waals interaction between phenol and (AC)-CHO. The adsorption energy is 7.107 kJ/mol^{-1}. If dispersion energy is excluded, the adsorption energy becomes 19.489 kJ/mol^{-1}, indicating a repulsive interaction between the phenol molecule and the surface of (AC)-CHO. This means that the adsorption of phenol on CHO-functionalized AC is unfavorable.

Table 2 Adsorption energies (kJ/mol^{-1}) and distances (D) between the adsorbate and adsorbent for phenol adsorption on functionalized AC

System	Interaction mode	E_{ads} (kJ/mol^{-1})	D (Å)
C_6H_5OH + (AC)-OH	$(C_6H_5)OH\cdots OH(AC)$	8.291	1.908
	$(C_6H_5)HO\cdots HO(AC)$	−30.736	1.689
C_6H_5OH + (AC)-CHO	$(C_6H_5)OH\cdots OCH(AC)$	7.107	1.803
C_6H_5OH + (AC)-COOH	$(C_6H_5)OH\cdots HOOC(AC)$	−17.769	1.784

Phenol adsorption on (AC)-COOH

The interaction between C_6H_5OH and the functional group –COOH of (AC)-COOH was found to lead to the complex $(C_6H_5)OH\cdots HOOC(AC)$ (Fig. 5b) and the formation of two hydrogen bonds: one between the H atom of the OH group of C_6H_5OH and the O atom of the –COOH group (with a bond distance of 2.250 Å) and the other between the O atom of the OH group of C_6H_5OH and the H atom of the –COOH group (with a bond distance of 1.784 Å). The weak adsorption energy of this interaction mode (−17.769 kJ/mol^{-1}, which is less negative than that for the $(C_6H_5)HO\cdots HO(AC)$ complex) suggested that it corresponded to physisorption. A possible explanation for this is that the presence of the carboxylic group affected physical adsorption. Carboxylic groups act as electron acceptors, causing a decrease in the π-electron density in the carbon planes, which leads to a decrease in the strength of the interactions between the aromatic ring of the phenol molecule and the carbon basal planes (resulting in

Table 3 Some structural parameters of C_6H_5OH and (AC)-OH

	C_6H_5OH	(AC)-OH
r(O–H) in	0.982	0.984
O–H stretching frequency in cm^{-1}	3634.6 (3656)[a]	3592.7

[a] Taken from experimental data [45]

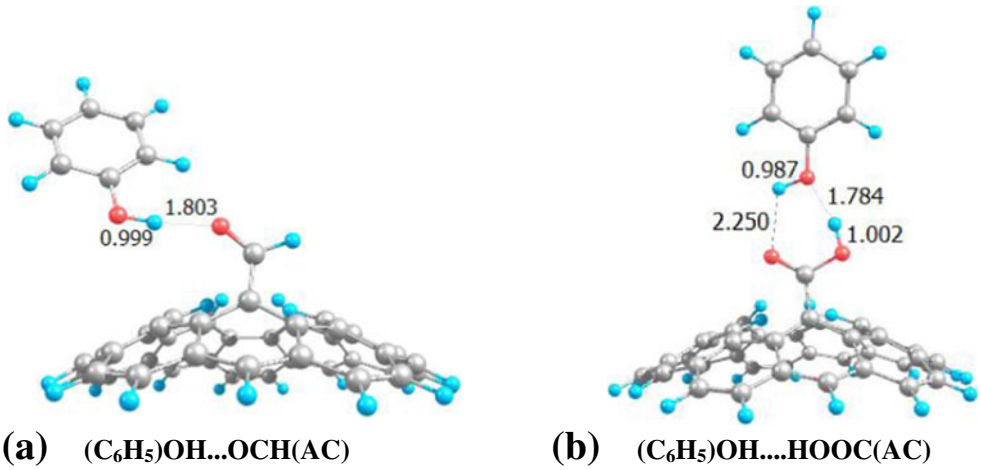

Fig. 5a–b The final configurations for the adsorption of C_6H_5OH on (AC)-CHO (**a**) and on (AC)-COOH (**b**)

weaker van der Waals interactions). The overall effect of this was a decrease in the average energy of adsorption sites. If the van der Waals energy is excluded, the adsorption energies associated with the $(C_6H_5)HO\cdots HO(AC)$ and $(C_6H_5)OH\cdots HOOC(AC)$ interactions change to −6.976 for $(C_6H_5)HO\cdots HO(AC)$ and −7.311 kJ/mol^{-1} for $(C_6H_5)OH\cdots HOOC(AC)$.

In the $(C_6H_5)OH\cdots HOOC(AC)$ complex, the O–H bond lengths in both C_6H_5OH and (AC)-COOH increased from 0.982 Å to 0.987 Å and from 0.988 Å to 1.002 Å, respectively. On the other hand, the stretching frequencies of the O–H bonds in C_6H_5OH and (AC)-COOH decreased from 3634.6 and 3575.4 cm^{-1} in the isolated molecules to 3577.1 and 3300.3 cm^{-1} in the complexes, respectively.

Conclusions

We studied the adsorption of phenol on pristine AC and AC functionalized with –OH, –CHO, and –COOH groups by performing density functional theory calculations. In our calculations, the fullerene-related structure was chosen for the model of activated carbon, and the AC surface was assumed to consist of curved fragments.

Four different interaction modes with the pristine AC were considered: interactions between the –OH group of phenol and each side of the AC surface (the convex and concave sides), and interactions of the aromatic ring with each of these sides of the AC surface. According to the results of our calculations, only a weak van de Waals interaction occurs between phenol and the pristine AC, which resulted in only very weak physical adsorption of phenol. Therefore, pristine AC is not able to bind phenol strongly enough to remove it from polluted water. However, the interaction of the aromatic ring with the convex side of the AC surface leads to quite a high dispersion energy, suggesting that phenol is adsorbed at sites that are large enough to accommodate it, and that the maximum heat due to the dispersive interactions is only released when adsorption occurs in pores that are similar in size to the phenol molecules.

Functionalization of the AC surface influences the phenol adsorption behavior of AC. Among the three functional groups that were used to functionalize the surface (–OH, –CHO, and –COOH), only interactions between the hydroxyl group of the phenol and OH-(AC) or HOOC-(AC) were found to lead to significant adsorption of phenol on the AC surface. Over (AC)-CHO, the interaction between the –OH group of phenol and the –CHO group was unfavorable, indicating very weak physical adsorption of phenol on the AC-CHO surface. Therefore, the results of our study suggest that functionalization does not always increase the adsorption capacity of AC. However, AC can be functionalized with functional groups that enhance its interactions with the adsorbate, hence improving its adsorption properties.

Acknowledgments This work was supported by the Ministry of Training and Education under project number B2011-17- 03. The authors appreciate the financial support from grants B2011-17-03.

References

1. Fierro V, Torne-Fernandez V, Montane D, Celzard A (2008) Microporous Mesoporous Mater 111:276
2. Aksu Z, Yener J (2001) Waste Manage 21:695
3. Park KH, Balathanigaimani MS, Shim WG, Lee JW, Moon H (2010) Microporous Mesoporous Mater 127:1
4. Dursun G, Cicek H, Dursun A (2005) J Hazard Mater B125:175
5. Goncharuk VV, Kucheruk DD, Kochkodan VM, Badekha VP (2002) Desalination 143:45
6. Kojima T, Nishijima K, Matsukata M (1995) J Membr Sci 102:43
7. Kujawski W, Warszawski A, Ratajczak W, Porebski T, Capala W, Ostrowska I (2004) Desalination 163:287
8. Rengaraj S, Moon SH, Sivabalan R, Arabindoo B, Murugesan V (2002) Waste Manage 22:543
9. Bansal RC, Donnet JB, Stoeckli F (1988) Active carbon. Dekker, New York
10. Boehm HP (1966) Advances in catalysis, vol 16. Academic, New York

11. Puri BR (1970) In: Walker PJ (ed) Chemistry and physics of carbon, vol 6. Dekker, New York
12. Marsh H, Heintz EA, Rodriguez-Reinoso F (eds) (1997) Introduction to carbon technologies. University of Alicante, San Vicente del Raspeig
13. Avgul NN, Kiselev AV (1970) In: Walker PJ (ed) Chemistry and physics of carbon, vol 6. Dekker, New York
14. Adib F, Bagreev A, Bandosz TJ (1999) J Colloid Interface Sci 216:360
15. Adib F, Bagreev A, Bandosz TJ (2000) Langmuir 16:1980
16. Bandosz TJ, Jagiello J, Schwarz J (1993) Langmuir 9:2518
17. Salame II, Bandosz TJ (2003) J Colloid Interface Sci 264:307
18. Leng CC, Pinto NG (1997) Carbon 35:1375
19. Tessmer TH, Vidic RD, Uranowski LJ (1997) Environ Sci Technol 31:1872
20. Franklin RE (1951) Proc R Soc A 209:196
21. Harris PJF, Burian A, Duber S (2000) Phil Mag Lett 80:381
22. Harris PJF (2005) Crit Rev Solid State Mater Sci 30:235
23. Zetterstrom P, Urbonaite S, Lindberg F, Delaplane RG, Leis J, Svensson G (2005) J Phys Condens Matter 17:3509
24. Hawelek L, Koloczek J, Brodka A, Dore JC, Honkimaeki V, Burian A (2007) Phil Mag 87:4973
25. Harris PJF (2008) J Phys Condens Matter 20:362201
26. Padak B, Wilcox J (2009) Carbon 47(12):2855
27. Chen N, Yang RT (1998) Carbon 36:1061
28. Chen N, Yang RT (1998) J Chem Phys A 102:6348
29. Lamoen D, Persson BNJ (1998) J Chem Phys 108:3332
30. Zhu ZH, Lu GQ (2004) Langmuir 20:10751
31. Janiak C, Hoffmann RR, Sjovall P, Kasemo B (1993) Langmuir 9:3427
32. Pliego JR, Resende SM, Humeres E (2005) J Chem Phys 314:127
33. Thomson KT, Gubbins KE (2000) Langmuir 16:5761
34. Terzyk AP, Furmaniak S, Gauden PA, Harris PJF, Włoch J, Kowalczyk P (2007) J Phys Condens Matter 19:406208
35. Terzyk AP, Furmaniak S, Harris PJF, Gauden PA, Włoch J, Kowalczyk P, Rychlicki G (2007) Phys Chem Chem Phys 9:59195
36. Perdew JP, Burke K, Ernzerhof M (1996) Phys Rev Lett 77:3865
37. Klamt A, Schüürmann G (1993) J Chem Soc Perkin Trans 2 5:799–805
38. Wu X, Vargas MC, Nayak S, Lotrich V, Scoles G (2001) J Chem Phys 115:8748
39. Grimme S (2006) J Comput Chem 27:1787
40. Zhao X, Gao B, Cai QH, Wang XG, Wang XZ (2011) Theor Chem Accounts 129:85
41. Peyghan AA, Baei MT, Moghimi M, Hashemian S (2012) Comput Theor Chem 997:63
42. Rokhina ER, Lahtinen M, Makarova K, Jegatheesan V, Virkutyte J (2012) Bioresour Technol 113:127–131
43. Moreno-Castilla C, Ferro-Garcia MA, Joly JP, Bautista-Toledo I, Carrasco-Marin F, Rivera-Utrilla J (1995) Langmuir 11:4386–4392
44. Díaz E, Ordóñez S, Vega A (2007) J Colloid Interface Sci 305:7–16
45. Michalska D et al (2001) J Phys Chem A 105:8734–8739